Title

Trapping the Complex Molecular Machinery of Polyketide and Fatty Acid Synthases with Tunable Silylcyanohydrin Crosslinkers

Journal

Angewandte Chemie International Edition, 57(52)

ISSN

1433-7851

Authors

Konno, Sho

La Clair, James J

Burkart, Michael D

Publication Date

2018-12-21

DOI

10.1002/anie.201806865

Peer reviewed

HHS Public Access

Author manuscript

Angew Chem Int Ed Engl. Author manuscript; available in PMC 2019 December 21.

Published in final edited form as:

Angew Chem Int Ed Engl. 2018 December 21; 57(52): 17009–17013. doi:10.1002/anie.201806865.

Trapping the complex molecular machinery of polyketide and fatty acid synthases with tunable silylcyanohydrin crosslinkers

Sho Konno[a], **James J. La Clair**[a], and **Michael D. Burkart**[a]

[a]Department of Chemistry and Biochemistry, University of California, San Diego, 9500 Gilman Drive, La Jolla CA 92093-0358

Abstract

Many families of natural products are synthesized by large multidomain biological machines commonly referred to as megasynthases. While the advance of mechanism-based tools has opened new windows into the structural features within the protein • protein interfaces guiding carrier protein dependent enzymes, there is an immediate need for tools that can be engaged to link co-translated domains in a site-selective manner. Here, we demonstrate the use of silylcyanohydrins in a two-step, two-site selective crosslinking for the trapping of carrier protein interactions within megasynthases. This advance provides a new tool to trap intermediate states within multimodular systems, a key step toward understanding the specificities within fatty acid (FAS) and polyketide (PKS) synthases.

Graphical Abstract

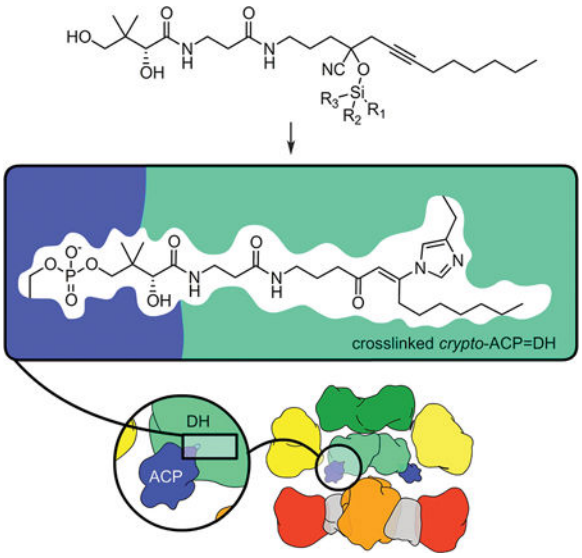

Mechanism based crosslinking is a vital tool to trap states within multimodular enzymatic systems. Here, we describe a caged system that applies silylcyanohydrin chemistry to mask a

Dedicated to Gilbert Stork

Supporting information including experimental procedures, synthetic methods and compound characterization has been provided. This data can be found via a link at the end of the document.

reactive ketone warhead. Given the diversity of different silyl groups, we demonstrate how this system can be tuned to deliver high yields of protein • protein crosslinking as defined in the context of large polyketide and fatty acid synthases.

Keywords

protein crosslinking; protein labeling; synthases; biosynthesis; natural products

The parallel development of protein crosslinkers and technical advances in mass spectroscopy, NMR, X-ray crystallography or cryo-EM continues to be vital to establishing a mechanistic understanding of Nature's biomacromolecular machines.[1] Protein crosslinking has played a critical role in stabilizing dynamic multi-protein complexes to enable the structural evaluation of these systems.[2] To date, the methods of chemical or enzymatic crosslinking between two proteins have involved selective reactions between amino acid side chains of each protein.[3] Unfortunately, these tools cannot always selectively engage a specific step within the mechanical motion of a biomolecular machine or temporally control reactivity.[4] This can be problematic for highly modular systems including fatty acid synthases (FAS)[5] and polyketide synthases (PKS),[6] which catalyze multiple chemical steps (Fig. 1).

In our previous studies, we developed a dehydratase (DH) specific probe for trapping an AcpP • FabA (DH) complex of the *Escherichia coli* FAS.[7] Here, **1** containing a 3-alkynylsulfone warhead (Fig. 2) was chemoenzymatically attached to AcpP. The reactive conjugate was purified and then introduced to FabA, in which an active site His selectively reacted with the warhead, generating an electrophilic allene trap *in situ* (Supporting Fig. S1a). While effective with type II synthases, the methodology translated poorly to type I systems. In type II systems, the acyl carrier protein (ACP) can be labeled first and then the DH is introduced. Experimentally, excess DH is added to achieve reaction completion. However in type I systems the ACP and DH domains are present at a fixed 1:1 stoichiometry. Presenting an ACP and DH reactive probe would mean that the crosslinking mechanism could begin with ACP loading and end with DH crosslinking, or alternatively begin with DH reactivity and end with ACP crosslinking. While DH crosslinking occurs without exogenous catalysis, the ACP loading process requires a complex enzymatic activation, one that is very unlikely to effectively occur once an agent has been attached to the DH in a type I synthase. To establish control, we developed a system that could load the *apo*-ACP to its corresponding *crypto*-ACP with an unreactive masked warhead, and then subsequently reveal the warhead when appropriate. Through this improved control, this strategy could also allow the adoption of more reactive warheads and potentially enable the crosslinking of protein partners with lower affinity.

To explore this issue, we turned to the mycocerosic acid synthase (MAS), a model system that contains six discrete enzymes (Fig. 1).[8] For the production of a molecule of mycocerosic acid (Fig. 1a), each of these enzymes conducts a choreographed operation of chain elongation and tailoring (Fig. 1b-1c). Recently, the structure of an MAS-like PKS have been solved.[9] Although ACP was excluded in this study, the overall model obtained by

combining structures of the two component regions in this study revealed the domain organization (Fig. 1c).

In the 1970s, the recognition that protons could be replaced by silicon offered a robust new approach to synthetic methodology,[10] as exemplified by the introduction of the TBS protecting group by Stork then Corey.[11] The utility of silicon became even more apparent a year later when Mukaiyama demonstrated the ability to condense silyl enol ethers with aldehydes or ketones, thereby solving the fundamental regioselective issue associated with the aldol condensation.[12] While accepted synthetically, silicon has not gained similar applicability in chemical biology.

We turned to silylcyanohydrins **3**-**5** as masked surrogates of the DH crosslinker **1** to test this hypothesis.[13] Here, the installation of a cyanohydrin in **8**-**11** (pKa ~25) ablated the acidic protons adjacent to the sulfone in **6** (pKa 12–14) or ketone in **7** (pKa 10–11). As illustrated in Scheme 1, we anticipated that **3**-**5** could be coupled to the appropriate ACP using a one pot chemoenzymatic method.[14] Once appended, the reactive unit of the resulting *crypto*-ACP **12** could be revealed by addition of fluoride to afford the corresponding cyanohydrin *crypto*-ACP **13** in the presence of a DH. Cyanohydrin **13** can then bind to the DH, forming complex **14**. Loss of HCN would generate ketone **15**, which is set to trap a proximal His residue (Supporting Fig. S1b) and form crosslinked **16**.[15]

Our plan was to first use the fluorescent probes **6**-**11**[16] to optimize covalent modification of the DH (**15**-**16**, Scheme 1) and then return to **3**-**5** to implement the crosslinking process (Scheme 1). Adapting established methods for pantetheinamide synthesis,[17] we prepared samples of silylcyanohydrin crosslinkers **3**-**5** and fluorescent probes **9**-**11** (Fig. 2) along with **1** (alkynyl sulfone for comparison), **2** (a control lacking the pantetheine arm) and **6**-**8** (non-silylcyanohydrin probes for comparative purposes). We first conducted labeling experiments of recombinant *E. coli* FabA (DH) with **6**-**11** to demonstrate the mechanism-based labeling. As shown in Fig. 3a, ketone **7** showed strong labeling compared with 3-alkynylsulfone **6** under the same conditions.

The specific labeling of the active site of FabA was confirmed by competitive experiments with pre-incubation of inhibitor **2** (Fig. 3a). Comparable labeling was also observed when using cyanohydrin **8** or TMS **9**, while DMES **10** and TES **11** showed negligible labeling (Fig. 3a). In addition, alcohol **S21** showed no labeling of FabA (Fig. S3). This result indicates that the alkynyl ketone warhead was essential for FabA labeling.

Next, we tested the deprotection of the silyl group by the addition of fluoride (Fig. 3b). FabA treated with ketone **7** in the presence or absence of fluoride exhibited the same labeling intensity, which indicates that addition of KF has no influence on FabA labeling. The increased labeling of FabA by KF was observed in DMES **10** and TES **11**, with **10** demonstrating the optimal activity. The TMS **9** was too unstable and underwent spontaneous deprotection and labeling without the addition of fluoride.

Further evaluation of these cyanohydrins provided stronger support for their selectivity. Although sulfone **6** could only label FabA at basic pH 8.0–8.5,[16] ketone **7** and cyanohydrin

8 operated at 5.0–8.5 (Fig. 3c). In addition, stability and deprotection of **10** with KF was not affected by pH. The complete deprotection of the DMES group was achieved with 100 mM KF (Supporting Fig. S4). In addition to pH screening, time-course studies allowed us to determine that the optimal labeling of FabA occurred within 8 h (Supporting Fig. S5). These studies now show that active site reactivity can be restrained until ACP loading through selective warhead caging.

We then asked whether **6**-**11** could selectively label DH domains in protein mixtures. As shown in Fig. 3d, ketone **7** and DMES **10** selectively-labeled FabA in a mixture of six *E. coli* FAS proteins AcpP (ACP, b6, Fig. 3d), FabA, FabD (MAT, b3, Fig. 3d), FabF (KS, b2, Fig. 3d), FabG (KR, b5, Fig. 3d) and FabI (ER, b4, Fig. 3d). While the labeling of FabA (b1, Fig. 3d) was inhibited by the addition of the reactive control **2,** this was accompanied by a non-selective labeling of FabF. Similar selectivity was observed when exploring *E. coli* K12 lysates spiked with recombinant FabA (b1, Fig. 3e-3f). Interestingly, we were able to visualize labeling of FabA with **7** and **10**, but not **6** (Fig. 3e-3f). The uncaging of **10** was found to be the most effective with minimal background and high yield.

After using the fluorescent system to tune DH labeling, we turned our attention to crosslinking. Our studies began by examining the efficacy of loading **1**, DMES **3**, TES **4** or TBS **5** onto AcpP (8.6 kDa), followed by sequential crosslinking to FabA (19 kDa). As shown in Fig. 4a, **1** and **3** crosslinked with or without KF. The bulkier **5** loaded, but its reaction with KF was slow. The intermediately sized **4** underwent effective loading onto AcpP (Fig. S6), followed by sequential crosslinking to FabA. Interestingly, this study demonstrated that the steric environment around the silicon atom can be used to tailor crosslinking.

We then examined the ability to crosslink other ACPs and a peptidyl carrier protein, PltL, to FabA. As shown in Fig. 4b, crosslinked bands were observed from ACP4 (20 kDa),[18] actACP (9.2 kDa)[19] and PltL (10 kDa).[20] Based on gel densitometry, the yield of these unoptimized reactions was 52±3%, 36±2%, and 15±3% for FabA=AcpP, FabA=actACP and FabA=PltL, respectively. Except for AcpP=FabA, this crosslinking was only possible when using **4** and triggering with KF. Comparable results were also observed for DH4 (33 kDa) [21] with its cognate ACP4. ACP4=DH4 (Fig. 4c) was readily formed, but crosslinking was only weakly observed for the unnatural pairings of AcpP=DH4, act-ACP=DH4 and PltL=DH4 (Fig. 4c).[22]

Finally, we applied these crosslinkers to MAS (226 kDa), a type I PKS (Fig. 4d). Crosslinkers **1**, **3**, **4** or **5** were loaded onto the ACP in MAS, then the warhead was revealed by addition of KF allowing for crosslinking to DH. Sulfone **1** showed no crosslinking product. Silylcyanohydrins **3**, **4** and **5** with or without KF acted similarly in crosslinking of AcpP=FabA. Notably, TES **4** returned 45±3% of intramolecularly crosslinked ACP=DH in MAS in media containing KF (Fig. S8), while the silyl-group reacted either too rapidly for DMES **3** or too slow for TBS **5**.

This discovery enables the development of silicon-caged crosslinking agents that can be tuned to selectively induce site-specific crosslinks by the addition of fluoride. Studies are

now underway to advance this tool for structural biology applications. It is likely that the ability to selectively deprotect silyl groups (TES *versus* TBS [23] at different rates adds immediate value for a wide array of protein • protein binding surveys. Finally, we suggest that the application of silicon in chemical biology is an untapped resource that offers a wide array of new and vital tools for addressing both systems-wide and structural queries.

Supplementary Material

Refer to Web version on PubMed Central for supplementary material.

Acknowledgements

We thank Drs. Anthony Mrse, Maj Ghassemian and Yongxuan Su for assistance with acquisition of NMR and MS data. DEBS ACP4 and DH4 constructs were graciously provided by Prof. Adrian Keatinge-Clay (UT Austin). This research was supported by a grant from the NIH (GM-095970). S. K. was supported in part by a fellowship from The Uehara Memorial Foundation.

References

[1]. a) Carroni M, Saibil HR, Methods 2016, 95, 78–85; [PubMed: 26638773] b) Basquin J, Taschner M, Lorentzen E, Adv. Exp. Med. Biol 2016, 896, 305–314. [PubMed: 27165333]

[2]. a) Leitner A, Faini M, Stengel F, Aebersold R, Trends Biochem. Sci 2016, 41, 20–32; [PubMed: 26654279] b) Cuniasse P, Tavares P, Orlova EV, Zinn-Justin S, Curr. Opin. Struct. Biol 2017, 43, 104–113; [PubMed: 28056362] c) Smits AH, Vermeulen M, Trends Biotechnol 2016, 34, 825–834. [PubMed: 26996615]

[3]. a) Artigues A, Nadeau OW, Rimmer MA, Villar MT, Du X, Fenton AW, Carlson GM, Adv. Exp. Med. Biol 2016, 919, 397–431; [PubMed: 27975228] b) Sinz A, Arlt C, Chorev D, Sharon M, Protein Sci 2015, 24, 1193–1209; [PubMed: 25970732] c) Heck T, Faccio G, Richter M, Thöny-Meyer L, Appl. Microbiol. Biotechnol 2013, 97, 461–475. [PubMed: 23179622]

[4]. Recent studies on large machines such as the spliceosome provides an excellent example: a) Sperling J, Sperling R, Methods 2017, 125, 70–83; [PubMed: 28412289] b) Shi Y, Nat. Rev. Mol. Cell Biol 2017, 18, 655–670. [PubMed: 28951565]

[5]. a) White SW, Zheng J, Zhang YM, Rock CO, Annu. Rev. Biochem 2005, 74, 791–831; [PubMed: 15952903] b) Grininger M, Curr. Opin. Struct. Biol 2014, 25, 49–56. [PubMed: 24457260]

[6]. a) Bayly CL, Yadav VG, Molecules 2017, 22, 235. b) Weissman KJ, Nat. Chem. Biol 2015, 11, 660–670; [PubMed: 26284673] c) Khosla C, Herschlag D, Cane DE, Walsh CT, Biochemistry 2014, 53, 2875–2883. [PubMed: 24779441]

[7]. Nguyen C, Haushalter RW, Lee DJ, Markwick PR, Bruegger J, Caldara-Festin G, Finzel K, Jackson DR, Ishikawa F, O'Dowd B, McCammon JA, Opella SJ, Tsai SC, Burkart MD, Nature 2014, 505, 427–431. [PubMed: 24362570]

[8]. Gokhale RS, Saxena P, Chopra T, Mohanty D, Nat. Prod. Rep 2007, 24, 267–277; [PubMed: 17389997]

[9]. Herbst DA, Jakob RP, Zähringer F, Maier T, Nature 2016, 531, 533–537. [PubMed: 26976449]

[10]. Silcon in Organic Synthesis (Eds. Colvin EW, Baldwin JE, Buckingham AD, Danishefsky S), Butterworth and Co Ltd., London, 1981.

[11]. a) Stork G, Hudrlik PF, J. Am. Chem. Soc 1968, 90, 4462–4464; b) Corey EJ, Venkateswarlu A, J. Am. Chem. Soc 1972, 94, 6190–6191.

[12]. a) Kan SB, Ng KK, Paterson I, Angew. Chem. Int. Ed. Engl 2013, 52, 9097–9108; Angew. Chem. 2013, 125, 9267–9279; [PubMed: 23893491] b) Matsuo J, Murakami M, Angew. Chem. Int. Ed. Engl 2013, 52, 9109–9118; Angew. Chem. 2013, 125, 9290–9290. [PubMed: 23881865]

[13]. a) Kurono N, Yamaguchi M, Suzuki K, Ohkuma T, J. Org. Chem 2005, 70, 6530–6532. [PubMed: 16050725] b) Gregory RJH, Chem. Rev 1999, 99, 3649–3682. [PubMed: 11849033] c) Stork G, La Clair JJ, Spargo P, Nargund RP, Totah N, J. Am. Chem. Soc 1996, 118, 5304–5305.

[14]. Worthington AS, Burkart MD, Org. Biomol. Chem 2006, 4, 44–46. [PubMed: 16357994]

[15]. Endo K, Helmkamp GM, Jr., Bloch K, J. Biol. Chem 1970, 245, 4293–4296. [PubMed: 5498414]

[16]. a) Ishikawa F, Haushalter RW, Burkart MD, J. Am. Chem. Soc 2012, 134, 769–772; [PubMed: 22188524] b) Ishikawa F, Haushalter RW, Lee DJ, Finzel K, Burkart MD, J. Am. Chem. Soc 2013, 135, 8846–8849. [PubMed: 23718183]

[17]. Beld J, Cang H, Burkart MD, Angew. Chem. Int. Ed. Engl 2014, 53, 14456–14461. [PubMed: 25354391]

[18]. Wu N, Tsuji SY, Cane DE, Khosla C, J. Am. Chem. Soc 2001, 123, 6465–6474. [PubMed: 11439032]

[19]. Haushalter RW, Filipp FV, Ko KS, Yu R, Opella SJ, Burkart MD, ACS Chem. Biol 2011, 6, 413–418. [PubMed: 21268653]

[20]. Jaremko MJ, Lee DJ, Opella SJ, Burkart MD, J. Am. Chem. Soc 2015, 137, 11546–11549. [PubMed: 26340431]

[21]. Keatinge-Clay A, J. Mol. Biol 2001, 384, 941–953.

[22]. Although the alkyl chain of TES-cyanohydrin 4 is not the cognate length, it was accepted by the DEBS DH4.

[23]. Nelson TD, Crouch RD, Synthesis 1996, 1031–1069.

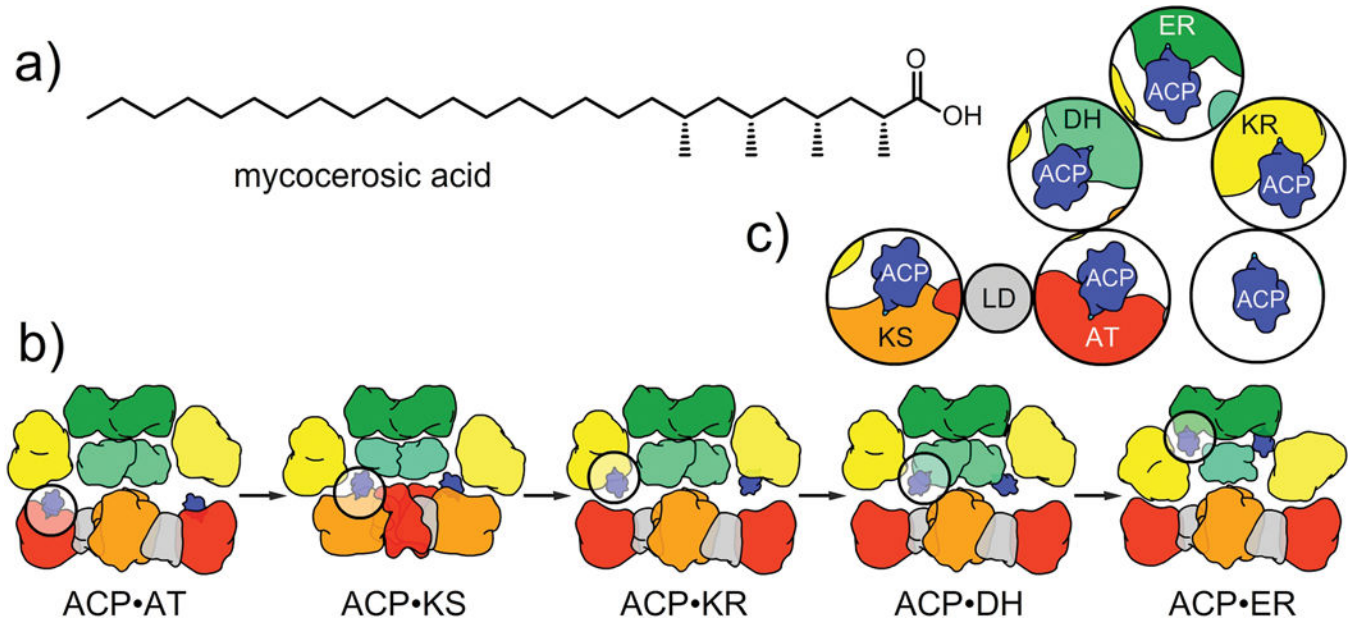

Figure 1.

Schematic representation of the mycocerosic acid synthase (MAS). **a)** Structure of mycocerosic acid. **b)** Steps involved in ketide processing in MAS. The acyl carrier protein (ACP, blue) interacts with five different domains sequentially beginning with the acyltransferase (AT, red) and ending with the enoyl reductase (ER, dark green) as different domains come in contact with the ACP (circles). **c)** An expansion of the MAS system depicting the AT, ACP, ketosynthase (KS, orange), ketoreductase (KR, yellow), dehydratase (DH, light green), and ER.

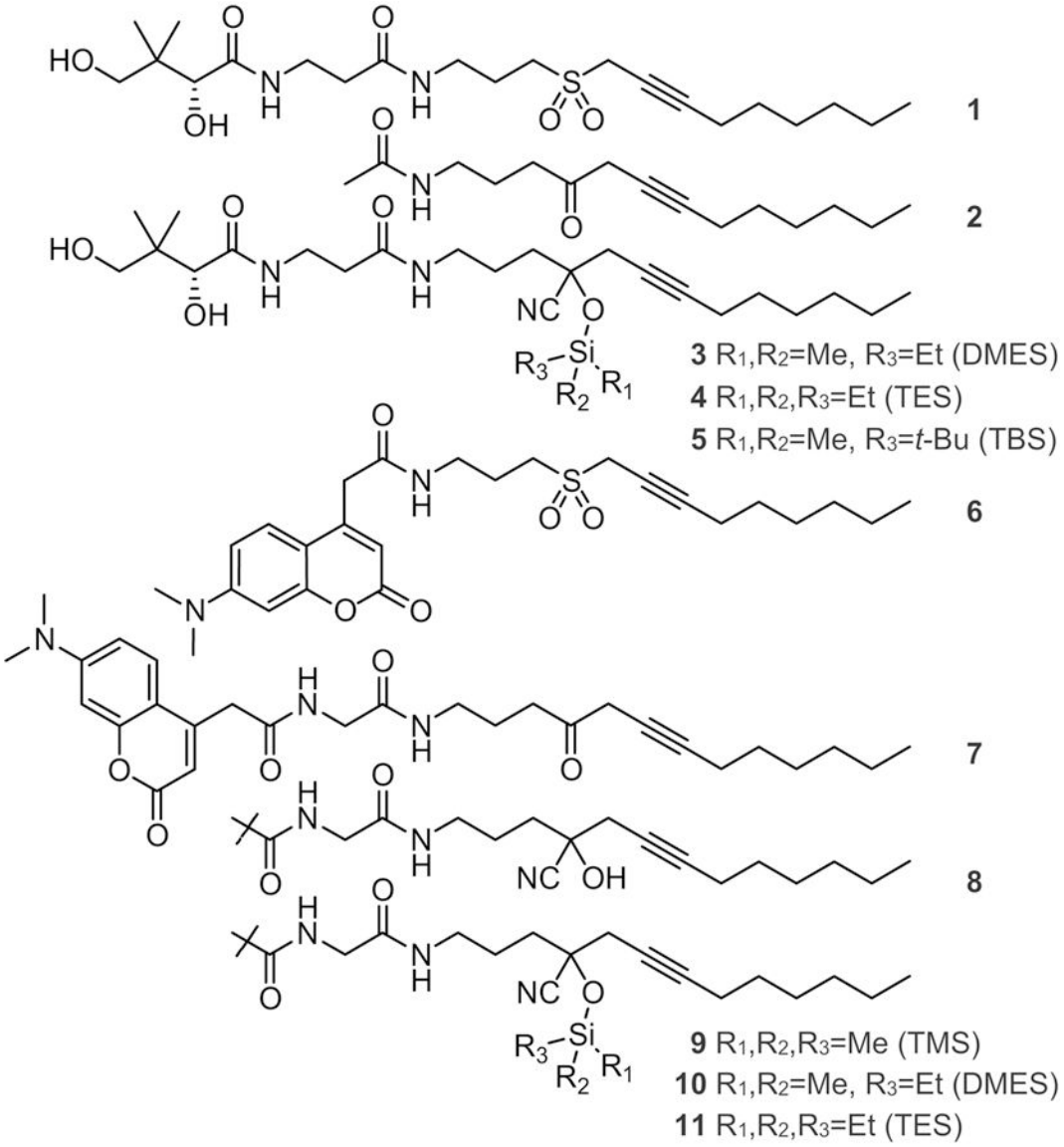

Figure 2.

Structures of crosslinking agents: sulfone **1**, dimethylethyl (DMES)-cyanohydrin **3**, triethylsilyl-(TES)-cyanohydrin **4**, and *t*-butyldimethylsilyl-(TBS)-cyanohydrin **5**. Inhibitor **2**, sulfone **6**, ketone **7**, cyanohydrin **8**, trimethylsilyl-(TMS)-cyanohydrin **9**, DMES-cyanohydrin **10**, and TES-cyanohydrin **11** were used for optimization. Studies with the glycine-linked equivalent of **6** (see **S23** in Fig. S2) were conducted to evaluate the role of the linker.

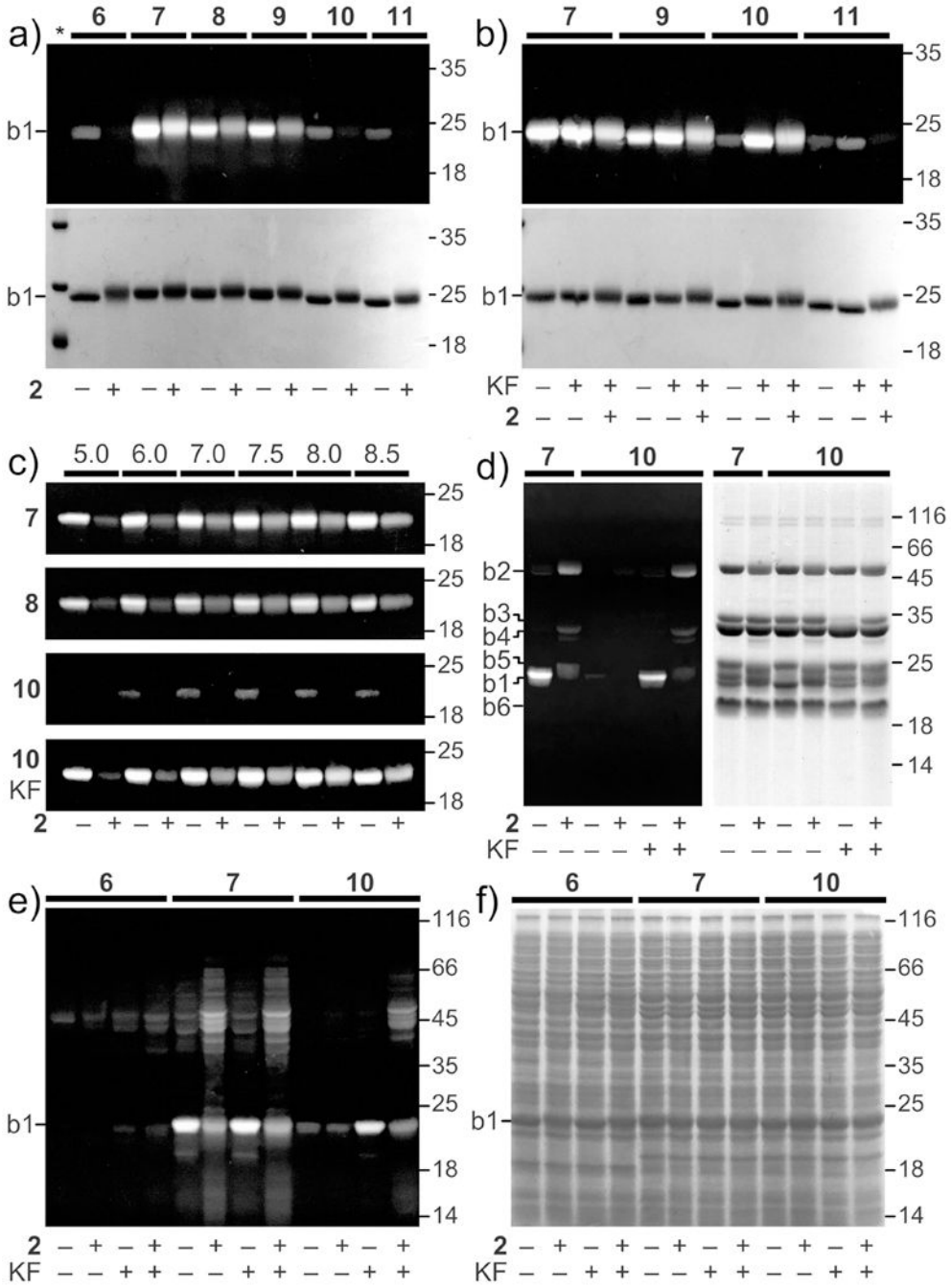

Figure 3.

Tunable fluorescent labeling of DH domains. **a)** A SDS-PAGE gel depicting the fluorescence (top) and total protein (bottom) from the incubation of 2 μM aliquot of FabA with 20 μM **6** at 37 °C, 2 μM **7** at 25 °C, 2 μM **8** at 25 °C, 2 μM **9** at 25 °C, 2 μM **10** at 25 °C or 2 μM **11** at 25 °C in 100 mM Tris•HCl pH 8.0 for 12 h. **b)** A SDS-PAGE gel depicting the fluorescence (top) and total protein (bottom) from the incubation of 2 μM aliquot of FabA with 2 μM **7,** 2 μM **9,** 2 μM **10** or 2 μM **11** at 25 °C for 12 h in 100 mM Tris•HCl pH 8.0 in the presence (+) or absence (–) of 100 mM KF. **c)** SDS-PAGE gels depicting the effects of

pH on the incubation of 2 μM FabA with 2 μM **7**, 2 μM **8**, or 2 μM **10** in 100 mM Tris•HCl at 25 °C for 12 h in the absence (–) or presence (+) of 100 mM KF. **d)** A SDS-PAGE gel depicting the fluorescence (left) and total protein (right) from the incubation of 2 μM of each protein with 2 μM **7** or 2 μM **10** in 100 mM Tris•HCl pH 7.0 at 25 °C for 12 h in the absence (–) or presence (+) of 100 mM KF. **e)** A SDS-PAGE gel depicting the fluorescence from the labeling of a 1.0 mg/mL aliquot of lysate from K12 *E. coli*, which was spiked with 2 μM FabA, and then treated with 20 μM **6** at 37 °C, 2 μM **7** at 25 °C, or 2 μM **10** at 25 °C in 100 mM Tris•HCl 150 mM NaCl pH 8.0 for 12 h in the absence (–) or presence (+) of 100 mM KF. **f)** Total protein stained gel in e). Protein bands are indicated by b1=FabA; b2=FabF; b3=FabD; b4=FabI; b5=FabG; and b6=AcpP. Comparison between reactions with and without 200 μM inhibitor **2** confirmed the site selectivity of the labeling. Supporting Fig. S7 provides full-scale gel images. Gel shifts were observed when appending **2**, **7**, **9** and **10** to FabA.

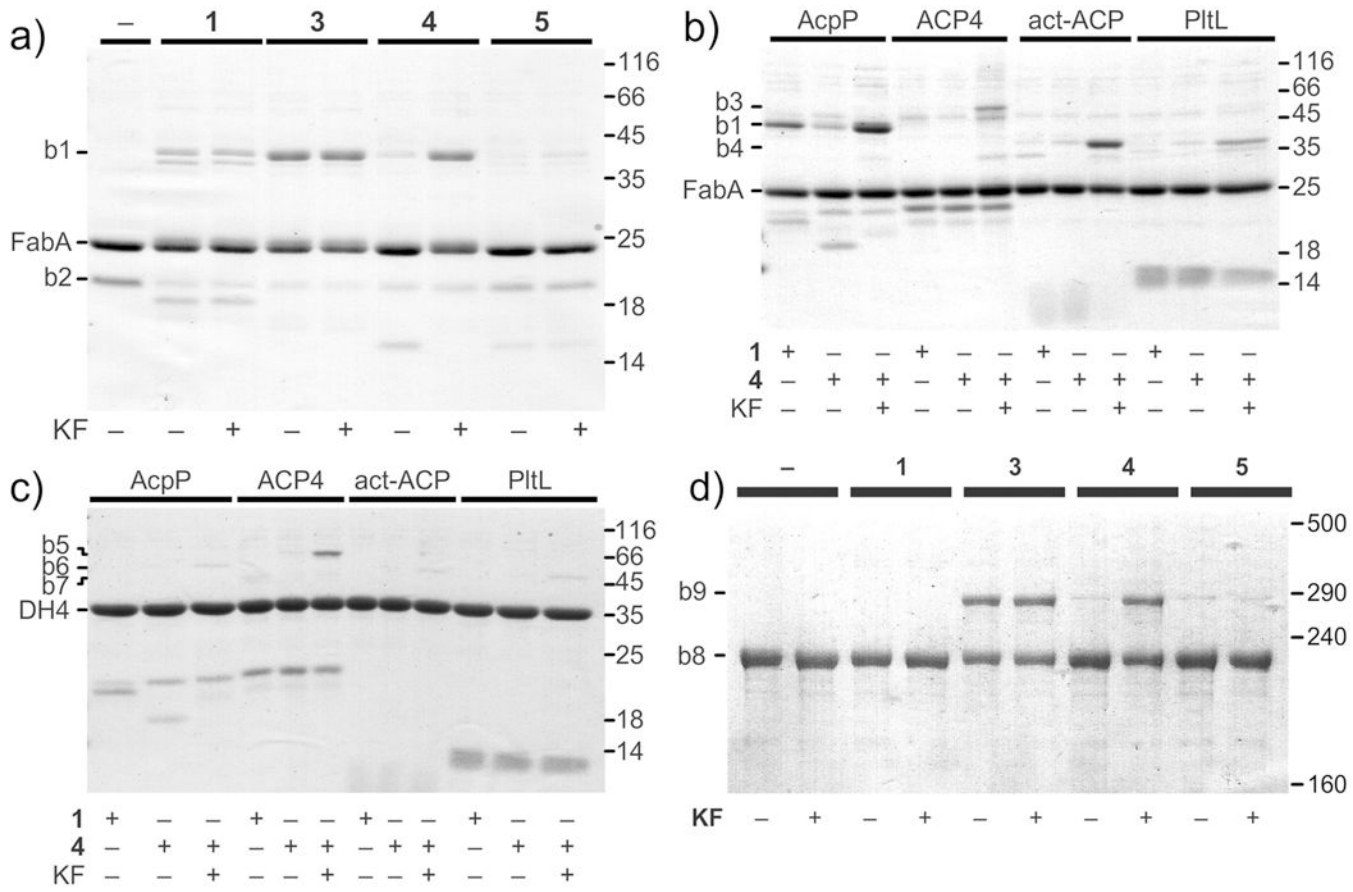

Figure 4.

Crosslinking studies. **a)** A SDS PAGE gel depicting 10 μM FabA that was incubated with 10 μM *crypto*-AcpP loaded with **1**, **3**, **4** or **5** in the absence (–) or presence (+) of 100 mM KF 50 mM Tris•HCl pH 8.5, 150 mM NaCl and 10% glycerol at 37 °C for 16 h. **b)** A SDS PAGE gel depicting 10 μM FabA that was incubated with 10 μM *crypto*-AcpP, 10 μM *crypto*-ACP4, 10 μM *crypto*-act-ACP or 10 μM *crypto*-PltL bearing either **1** or **4** in the absence (–) or presence (+) of 100 mM KF in 50 mM Tris·HCl pH 8.5, 150 mM NaCl and 10% glycerol at 37 °C for 24 h. **c)** A SDS PAGE gel depicting 10 μM DH4 that was incubated with 10 μM *crypto*-AcpP, 10 μM *crypto*-ACP4, 10 μM *crypto*-act-ACP or 10 μM *crypto*-PltL bearing either **1** or **4** in the absence (–) or presence (+) of 100 mM KF in 50 mM Tris•HCl pH 8.5, 150 mM NaCl and 10% glycerol at 37 °C for 24 h. **d)** SDS PAGE gel depicting 1 μM *apo*- or *crypto*-MAS loaded with **1**, **3**, **4** or **5** in the absence (−) or presence (+) of 100 mM KF 50 mM Tris•HCl pH 7.0, 150 mM NaCl and 10% glycerol at 25 °C for 12 h. Fig. S8 provides further support the intramolecular crosslinked species at 280 kDa. Bands are given by: b1=FabA=AcpP; b2=*holo*-AcpP; b3=FabA=ACP4; b4=FabA=*act*-ACP or FabA=PltL; b5=DH4=ACP4; b6=DH4=AcpP; b7 = DH4=act-ACP or DH4=PltL; b8 = *apo*- or *crypto*-MAS; or b9 = crosslinked *crypto*-MAS Supporting Fig. S7 provides full-scale gel images.

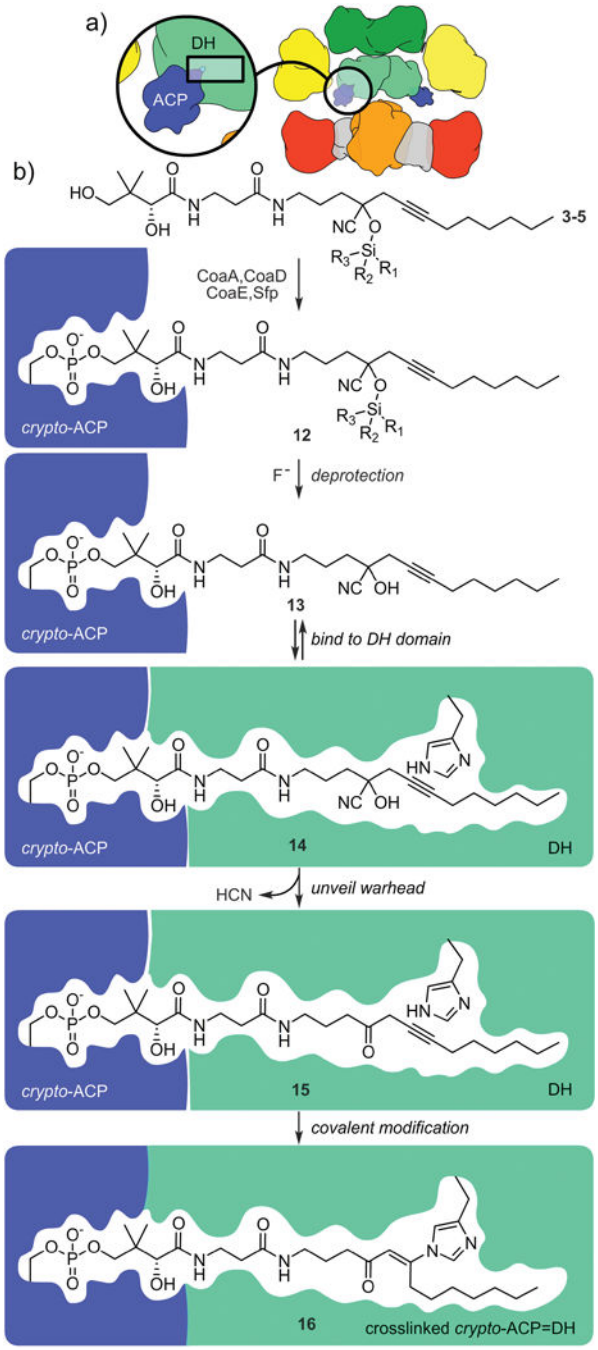

Scheme 1.

Silylcyanohydrin crosslinking. **a)** A view of a synthase undergoing an ACP•DH interaction, with a zoom onto the protein • protein interface (circle) and substrate binding pocket (square). **b)** Two-step silylcyanohydrin caged DH crosslinking. One pot loading of **3**-**5** onto the ACP results in *crypto*-ACP **12**, which can be purified and stored. The crosslinking reaction is induced by the addition of KF to a mixture of **12** and a DH. After deprotection, **13** binds to the DH and inserts its cargo into the DH active site, as shown in **14**. HCN is eliminated, and the resulting complex **15** can covalently modify proximal His residues

(Supporting Fig. S1).[15] Alternatively, the silylcyanohydrin in **12** can bind to the DH, and the subsequent steps could occur in the DH active site.